Reliable Assessment of Perfusivity and Diffusivity from Diffusion Imaging of the Body*

M. Freiman[1], S.D. Voss[2], R.V. Mulkern, J.M. Perez-Rossello[2], M.J. Callahan[2], and Simon K. Warfield[1]

[1] Computational Radiology Laboratory, Boston Children's Hospital, Harvard Medical School, MA, USA
[2] Department of Radiology, Boston Children's Hospital, Harvard Medical School, MA, USA

Abstract. Diffusion-weighted MRI of the body has the potential to provide important new insights into physiological and microstructural properties. The Intra-Voxel Incoherent Motion (IVIM) model relates the observed DW-MRI signal decay to parameters that reflect perfusivity (D^*) and its volume fraction (f), and diffusivity (D). However, the commonly used voxel-wise fitting of the IVIM model leads to parameter estimates with poor precision, which has hampered their practical usage. In this work, we increase the estimates' precision by introducing a model of spatial homogeneity, through which we obtain estimates of model parameters for all of the voxels at once, instead of solving for each voxel independently. Furthermore, we introduce an efficient iterative solver which utilizes a model-based bootstrap estimate of the distribution of residuals and a binary graph cut to generate optimal model parameter updates. Simulation experiments show that our approach reduces the relative root mean square error of the estimated parameters by 80% for the D^* parameter and by 50% for the f and D parameters. We demonstrated the clinical impact of our model in distinguishing between enhancing and nonenhancing ileum segments in 24 Crohn's disease patients. Our model detected the enhanced segments with 91%/92% sensitivity/specificity which is better than the 81%/85% obtained by the voxel-independent approach.

1 Introduction

Diffusion-weighted MRI (DW-MRI) of the body is a non-invasive imaging technique sensitive to the incoherent motion of water molecules inside the body. This motion is be a combination of the thermally-driven random motion of water molecules and blood flow in the randomly oriented tissue micro capillaries. These phenomena are characterized through the so-called, intra-voxel incoherent

* This investigation was supported in part by NIH grants R01 EB008015, R01 LM010033, R01 EB013248, and P30 HD018655 and by a research grant from the Boston Children's Hospital Translational Research Program.

N. Ayache et al. (Eds.): MICCAI 2012, Part I, LNCS 7510, pp. 1–9, 2012.

motion (IVIM) model with the diffusion (D), and the pseudo-diffusion (D^*) as the decay rate parameters, and the fractional contribution (f) of each motion to the DW-MRI signal decay [1,7].

IVIM model parameters have recently shown promise as quantitative imaging biomarkers for various clinical applications in the body, including differential analysis of tumors [4] and the assessment of liver cirrhosis [9]. However, IVIM parameter estimates are often unreliable, and thus are not widely utilized in the clinic [7]. Reliable estimates of IVIM model parameters are difficult to achieve because of 1) the non-linearity of the IVIM model, 2) the limited number of DW-MRI images as compared to the number of the IVIM model parameters; and 3) the low signal-to- noise ratio (SNR) observed in body DW-MRI.

While commonly used methods for IVIM parameter estimation fit the model to the signal at each voxel independently, they typically ignore the spatial context of the signal and thus produce highly unreliable estimates, especially for the pseudo-diffusion (D^*) and the fractional contribution (f) parameters [7]. In current practice, the DW-MRI signal is averaged over a region of interest (ROI) to increase the SNR, effectively yielding more reliable IVIM parameter estimates [12]. Unfortunately, by averaging the signal over a ROI, the estimated parameters do not reflect critical heterogeneous environments such as the necrotic and viable parts of tumors. An alternative approach is to average several DW-MRI acquisitions to increase the SNR [7]. While this retains the spatial sensitivity of the estimated parameters, it also increases the overall image acquisition time, which is not feasible in clinical practice. However, the overall image acquisition time increases, preventing this approach to be feasible in clinical practice.

Other groups have suggested incorporating spatial knowledge as a prior term to increase the reliability of parameters estimates in quantitative dynamic contrast enhanced MRI [6,10]. However, these models are difficult to optimize as compared to the simple voxel-wise approaches, and have not been successfully applied to incoherent motion quantification from body DW-MRI.

In this work, we increase the precision of the incoherent motion parameters estimates by introducing a model of spatial homogeneity, through which we obtain estimates of model parameters for all of the voxels at once, instead of solving for each voxel independently. Furthermore, we introduce an efficient iterative solver in order to obtain precise parameter estimates with this new model. Our solver utilizes a model-based bootstrap estimate of the distribution of residuals and a binary graph cut to generate optimal model parameter updates.

In our simulation experiments, we have shown a reduction in the relative root mean square (RRMS) error of parameter estimates in clinical SNR conditions by 80% for the D^* parameter and by 50% for the D and f parameters. In addition, we have assessed clinical impact, namely, the ability of incoherent motion parameters to distinguish enhancing from non-enhancing ileal segments in a study cohort of 24 Crohn's disease (CD) patients. Our results demonstrated that the incoherent motion parameters estimated with our method yielded a sensitivity of 91% and specificity of 92%, while the traditional voxel-independent approach only produced a sensitivity of 81% and specificity of 85%.

2 Method

2.1 DW-MRI Signal Decay Model

The IVIM model of DW-MRI signal decay assumes a function of the form [1]:

$$m_i = s_0 \left(f \exp(-b_i(D^* + D)) + (1 - f) \exp(-b_i(D))\right) \tag{1}$$

where m_i is the expected signal at b-factor=b_i, s_0 is the baseline signal (without any diffusion effect); f is the pseudo-diffusion fraction; D^* is the so-called, pseudo-diffusion coefficient characterizing the perfusion component; and D is the apparent diffusion coefficient associated with extravascular water.

Given the DW-MRI data acquired with multiple b-factors, the observed signal (S_v) at each voxel v is a vector of the observed signal at the different b-factors: $S_v = \{s_i\}, i = 1 \ldots N$. We model the IVIM model parameters at each voxel v as a continuous-valued four-dimensional random variable (i.e. $\Theta_v = \{s_0, f, D^*, D\}$). Taking a Bayesian perspective, our goal is to find the IVIM parametric maps $\hat{\Theta}$ that maximizes the posterior probability associated with the maps given the observed DW-MRI images (S) and the spatial prior knowledge ($p(\Theta)$):

$$\hat{\Theta} = \underset{\Theta}{\operatorname{argmax}}\, p(\Theta|S) \propto p(S|\Theta)p(\Theta) \tag{2}$$

By using a spatial prior in the form of a continuous-valued Markov random field, the posterior probability $p(S|\Theta)p(\Theta)$ decomposes into the product of maximal node and clique potentials:

$$p(S|\Theta)p(\Theta) \propto \prod_v p(S_v|\Theta_v) \prod_{v_p, v_q \in \Omega} p(\Theta_{v_p}, \Theta_{v_q}) \tag{3}$$

where Θ_v is the IVIM model parameters at voxel v, $p(S_v|\Theta_v)$ is the data term representing the probability of voxel v to have the DW-MRI signal S_v given the model parameters Θ_v, Ω is the collection of the neighboring voxels according to the employed neighborhood system, and $p(\Theta_{v_p}, \Theta_{v_q})$ is the spatial smoothness prior in the model.

The maximum *a posteriori* (MAP) estimate $\hat{\Theta}$ is then found by minimizing:

$$E(\Theta) = \sum_v \phi(S_v; \Theta_v) + \sum_{v_p, v_q \in \Omega} \psi(\Theta_{v_p}, \Theta_{v_q}) \tag{4}$$

where $\phi(S_v; \Theta_v)$ and $\psi(\Theta_{v_p}, \Theta_{v_q})$ are the compatibility functions:

$$\phi(S_v; \Theta_v) = -\log p(S_v|\Theta_v), \qquad \psi(\Theta_{v_p}, \Theta_{v_q}) = -\log p(\Theta_{v_p}, \Theta_{v_q}) \tag{5}$$

Assuming a noncentralized χ-distribution noise model for parallel MRI acquisition [3] as used in DW-MRI, the data term takes the following form:

$$\phi(S_v; \Theta_v) = -\sum_{i=1}^{N} \frac{m_i}{\sigma^2} + \log\left(\frac{m_i}{s_i}\right)^{n-1} - \left(\frac{m_i^2 + s_i^2}{2\sigma^2}\right) + \log I_{n-1}\left(\frac{s_i m_i}{\sigma^2}\right) \tag{6}$$

where s_i is the observed signal at b-factor b_i, m_i is the expected signal at b_i given the model parameters Θ_v calculated with Eq. 1, σ being the noise standard deviation of the Gaussian noises present on each of the acquisition channels, n being the number of channels used in the acquisition and I_{n-1} being the $(n-1)$th order modified Bessel function of the first kind.

The robust L1-norm is used as the spatial smoothness term:

$$\psi(\Theta_{v_p}, \Theta_{v_q}) = \alpha W |\Theta_{v_p} - \Theta_{v_q}| \tag{7}$$

where $\alpha \geq 0$ is the spatial coupling factor, and W is a diagonal weighting matrix which accounts for the different scales of the parameters in Θ_v.

2.2 Optimization Scheme

Direct minimization of the energy in Eq. 4 is a challenging optimization problem due to the very high dimensionality of the parameters vector Θ. For example a clinical 3D DW-MRI data of $192 \times 156 \times 40$ voxels would result in a parameter vector Θ of $\sim 5 \cdot 10^6$ dimensions.

To overcome this challenging optimization problem, we developed a new solver to robustly minimize the energy in Eq. 4.

Our "fusion bootstrap moves (FBM)" algorithm, inspired by the fusion-moves algorithm [8], iteratively applies the following two steps until the improvement in the optimized energy is smaller than some epsilon. First, we draw a new possible proposal of the incoherent motion model parameters values from the parameters distribution using model-based statistical bootstrapping [2]. Next, given the current assignment and the drawn sample, we use the binary graph-cut technique to fuse the two possible assignments of the IVIM values at each voxel in an optimal manner [8] to an assignment that reduces the model energy.

Since the fusion of the two possible proposals at each iteration is optimal, the reduction in the overall model energy (Eq. 4) is guaranteed. By applying the proposal drawing and optimal fusion steps iteratively, the algorithm will robustly converge, at least to a local minimum. We will describe these steps in detail next.

Proposal Drawing: We utilize the model-based bootstrap technique [2] to draw a new proposal from the empirical distribution of the incoherent motion parameters values as follows: For each voxel v, the raw residuals between the observed signal (S_v) and the expected signal ($M_v = \{m_i\}, i = 1, \ldots N$) at each b-factor b_i, given the current model estimate (Θ_v^0), are defined as: $\epsilon_i = m_i - s_i$. The model-based bootstrap resampling is defined as:

$$S_v^*(\Theta_v^0) = M_v + t_i \hat{\epsilon} \tag{8}$$

where $S_v^*(\Theta_v^0)$ is the resampled measures at the b-factors $b_i, i = 1 \ldots N$, $\hat{\epsilon}$ are the rescaled version of ϵ that accounts for heterogeneous error leverages [5], and t_i is a two-point Rademacher distributed random variable with $p(t = 1) = 0.5$ and $p(t = -1) = 0.5$ defined for each b-factor independently. The IVIM model parameters Θ_v^1 are then estimated for each voxel independently [7].

Binary Optimization: We use the binary graph-cut technique [8] to find the optimal combination of the current assignment Θ^0 and the new proposal Θ^1 for the IVIM model parameters values at each voxel as follows:

Let $G = (V, E)$ be an undirected graph, where each voxel v is represented as a graph node, the two proposals Θ^0 and Θ^1 are represented by the terminal nodes v_s and v_t, and graph edges consist of three groups: $E = \{(v_p, v_q), (v_p, v_s), (v_p, v_t)\}$.

Edge weights $w(v_p, v_s)$ and $w(v_p, v_t)$ represent the likelihood of the model parameters Θ^0 and Θ^1 given the observed signal S_{v_p}, respectively:

$$w(v_p, v_s) = \phi(S_v; \Theta_v^0), \qquad w(v_p, v_t) = \phi(S_v; \Theta_v^1) \tag{9}$$

Edge weights $w(v_p, v_q)$ penalize for adjacent voxels that have different model parameters: $w(v_p, v_q) = \psi(\Theta_{v_p}, \Theta_{v_q})$. The optimal fusion between Θ^0 and Θ^1 is then found by solving the corresponding graph min-cut problem. Finally, the result $\hat{\Theta}$ is assigned as Θ^0 for the next iteration.

3 Experimental Results

3.1 Simulation Experiment

We conducted a Monte-Carlo simulation study to analyze the estimation errors. We constructed a simulated heterogeneous tumor example [6] as follows. We defined three-dimensional reference parametric maps with $100 \times 100 \times 5$ voxels with the following parameters: Border: $\Theta = \{200, 0.35, 0.03, 0.003\}$, middle part: $\Theta = \{200, 0.25, 0.02, 0.002\}$, innermost part: $\Theta = \{200, 0.15, 0.01, 0.001\}$. We computed simulated DW-MRI images from the parametric maps using Eq. 1 with 7 b-values in the range $[0, 800]$ s/mm^2. We then corrupted the simulated data by noncentralized χ-distributed noise with single coil noise σ values of 2-16.

We estimated the model parameters $\hat{\Theta}$ from the noisy DW-MRI data for each voxel, using the voxel-independent approach (IVIM) [7] and using our model (IM). The optimization algorithm parameters were determined experimentally and were set as follows: α was set to 0.01, the rescaling matrix W diagonal was set to: $\{1.0, 0.001, 0.0001, 0.01\}$. The noise parameter σ was estimated using a pre-defined background region. Stopping criteria was defined as an energy improvement of less than 0.1% from the initial energy or 500 iterations. We calculated the RRMS error between the reference and estimated parameters [6].

Fig. 1 depicts the middle slice of the reference parametric maps and the model parameters estimates using the two methods along with the RRMS error of each estimator as a function of the $\mathrm{SNR}_{\mathrm{b0}}$ defined as the baseline signal s_0 divided by the noise level σ. Visually, the parametric maps computed using the IVIM model (2$^{\mathrm{nd}}$ column) exhibit very noisy estimates, in which the heterogeneous environment is hardly detectable, mainly for the D^* and f parameters (1$^{\mathrm{st}}$ and 2$^{\mathrm{nd}}$ rows). However, the maps computed using our IM method are much smoother, and the heterogeneous environment is more detectable. Quantitatively, our IM model decreases the overall RRMS of the D^* parameter by 80% and of the f and D parameters by 50% as compared to the IVIM model for $\mathrm{SNR}_{\mathrm{B0}} = 25$ which represents the actual noise level observed in clinical imaging studies.

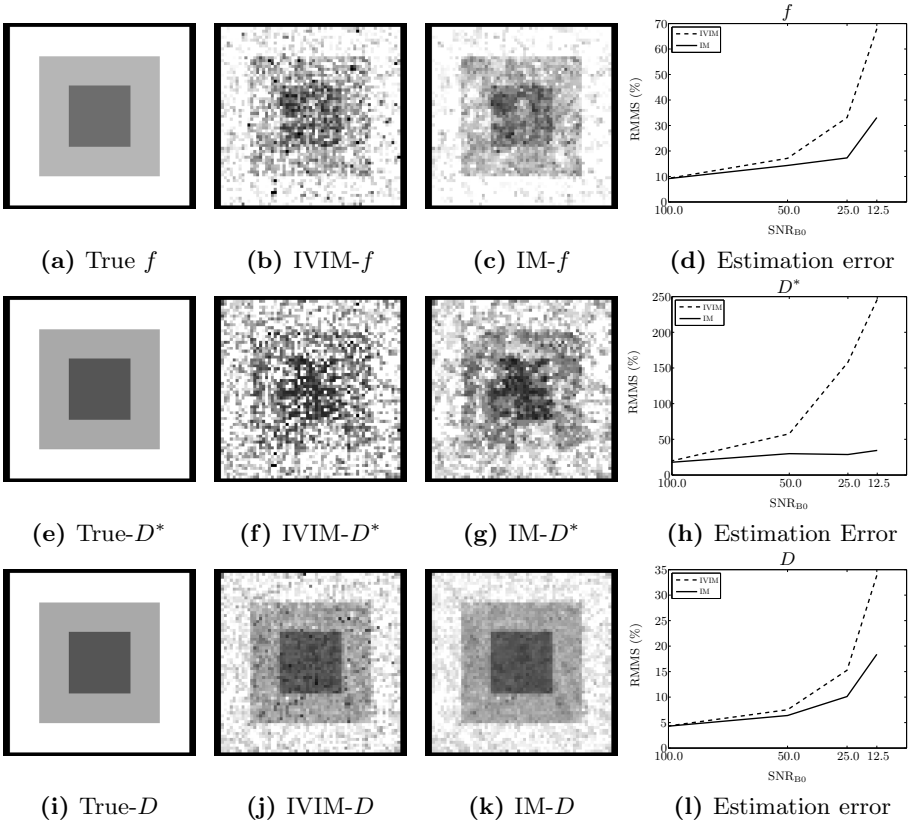

(a) True f **(b)** IVIM-f **(c)** IM-f **(d)** Estimation error

(e) True-D^* **(f)** IVIM-D^* **(g)** IM-D^* **(h)** Estimation Error

(i) True-D **(j)** IVIM-D **(k)** IM-D **(l)** Estimation error

Fig. 1. Simulated heterogeneous tumor example. The first column presents the "ground-truth" values used to simulate the DW-MRI data. The second and third columns present the estimated parameters using the IVIM, and our IM approaches, respectively. The fourth column presents the RRMS errors for each parameter for the different noise levels.

3.2 Clinical Impact

To demonstrate the actual clinical impact of using our IM model instead of the voxel-independent IVIM model, we assessed the discriminatory performance of the incoherent motion model parameters, in discerning enhancing from nonenhancing ileal segments of CD patients. CD is a chronic inflammatory disorder of the bowel, in which involvement of the ileum is common. Characterization of perfusivity and diffusivity in the ileum has a promising role in patient-specific management of the disease.

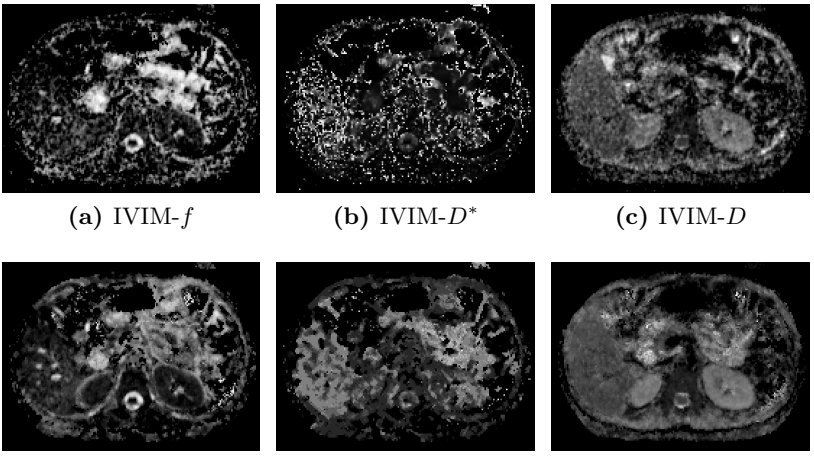

(a) IVIM-f **(b)** IVIM-D^* **(c)** IVIM-D

(d) IM-f **(e)** IM-D^* **(f)** IM-D

Fig. 2. Representative upper abdomen slice of the parametric maps reconstructed by the IVIM method (1st row), and by our method (2nd row). Our method yields smoother, more realistic maps, with sensitivity to details.

Table 1. Quantitative analysis of incoherent motion parameters for the nonenhancing and enhancing ileal segments. All values are in mean(std). Significant differences (two-tailed Student's t-test,n_1=11, n_2=13, $p<0.05$) are in bold.

	IVIM			**IM**		
	Nonenhancing	Enhancing	p-value	Nonenhancing	Enhancing	p-value
f	0.55 (0.24)	0.28 (0.16)	**0.004**	0.66(0.43)	0.32(0.15)	**0.02**
D^*	24.2(16.3)	36.1(20.6)	0.13	28.7(22.9)	42.5(32.7)	0.24
D	1.6 (0.6)	1.3 (0.4)	0.17	1.7(0.4)	1.2(0.3)	**0.002**

We acquired DW-MRI from 24 consecutive patients with confirmed CD using a 1.5-T unit (Magnetom Avanto, Siemens Medical Solutions, Erlangen, Germany). We performed free-breathing single-shot echo-planar imaging using the following parameters: repetition/echo time (TR/TE) = 6800/59 ms; matrix size = 192×156; field of view = 300×260 mm; slice thickness/gap = 5 mm/0.5 mm; 40 axial slices; 8 b-values = 5,50,100,200,270,400,600,800 s/mm^2. We defined reference standard classification of the ileal segments as the consensus of two independent radiologists' qualitative review of the clinical MR enterography data as enhancing (n=11) or nonenhancing (n=13). We fitted the signal-decay model to the DW-MRI using both the IVIM and IM approaches and we averaged the parameters values over the manually annotated ileum region.

Fig. 2 depicts a representative parametric maps of the upper abdomen. The IM model yields smoother, more realistic maps, especially for the f parameter.

Table 1 summarizes the measured values. The IM model was sensitive to the actual differences in both the tissue cellularity (D) and blood-flow (f) [11], while the IVIM model was not sensitive to the differences in tissue cellularity.

We constructed generalized linear models (GLM) from the parameters values to distinguish between enhancing and nonenhancing ileal segments. We assessed the sensitivity and specificity of the models by utilizing the optimal cutoff values calculated by ROC analysis of the GLM models. Our IM approach yield a sensitivity/specificity of 91%/92% while the IVIM approach yield only 81%/85%.

4 Conclusions

We have presented a new model and method for the reliable quantification of perfusivity and diffusivity from body DW-MRI that features the incorporation of spatial prior knowledge, with a new robust and accurate optimization technique. Our experiments demonstrated that our method reduces the estimates' RRMS substantially and improve the actual diagnostic accuracy of the incoherent motion parameters as compared to the voxel-independent approach.

References

1. Le Bihan, D., Breton, E., Lallemand, D., Aubin, M.L., Vignaud, J., Laval-Jeantet, M.: Separation of diffusion and perfusion in intravoxel incoherent motion MR imaging. Radiology 168(2), 497–505 (1988)
2. Davidson, R., Flachaire, E.: The wild bootstrap, tamed at last. J. of Econometrics 146(1), 162–169 (2008)
3. Dietrich, O., Raya, J.G., Reeder, S.B., Ingrisch, M., Reiser, M.F., Schoenberg, S.O.: Influence of multichannel combination, parallel imaging and other reconstruction techniques on mri noise characteristics. Magn. Reson. Imaging 26(6), 754–762 (2008)
4. Döpfert, J., Lemke, A., Weidner, A., Schad, L.R.: Investigation of prostate cancer using diffusion-weighted intravoxel incoherent motion imaging. Magn. Reson. Imaging 29(8), 1053–1058 (2011)
5. Freiman, M., Voss, S., Mulkern, R., Perez-Rossello, J., Warfield, S.: Quantitative Body DW-MRI Biomarkers Uncertainty Estimation Using Unscented Wild-Bootstrap. In: Fichtinger, G., Martel, A., Peters, T. (eds.) MICCAI 2011, Part II. LNCS, vol. 6892, pp. 74–81. Springer, Heidelberg (2011)
6. Kelm, B.M., Menze, B.H., Nix, O., Zechmann, C.M., Hamprecht, F.A.: Estimating kinetic parameter maps from dynamic contrast-enhanced mri using spatial prior knowledge. IEEE Trans. Med. Imaging 28(10), 1534–1547 (2009)
7. Koh, D.M., Collins, D.J., Orton, M.R.: Intravoxel incoherent motion in body diffusion-weighted mri: Reality and challenges. AJR Am. J. Roentgenol. 196(6), 1351–1361 (2011)
8. Lempitsky, V., Rother, C., Roth, S., Blake, A.: Fusion moves for markov random field optimization. IEEE Trans. Pattern Anal. Mach. Intell. 32(8), 1392–1405 (2010)
9. Luciani, A., Vignaud, A., Cavet, M., Van Nhieu, J.T., Mallat, A., Ruel, L., Laurent, A., Deux, J.F., Brugieres, P., Rahmouni, A.: Liver cirrhosis: intravoxel incoherent motion mr imaging–pilot study. Radiology 249(3), 891–899 (2008)

10. Schmid, V.J., Whitcher, B., Padhani, A.R., Taylor, N.J., Yang, G.Z.: Bayesian methods for pharmacokinetic models in dynamic contrast-enhanced magnetic resonance imaging. IEEE Trans. Med. Imaging 25(12), 1627–1636 (2006)
11. Targan, S., Shanahan, F., Karp, L.: Inflammatory bowel disease: from bench to bedside. Springer (2005)
12. Zhang, J.L., Sigmund, E.E., Rusinek, H., Chandarana, H., Storey, P., Chen, Q., Lee, V.S.: Optimization of b-value sampling for diffusion-weighted imaging of the kidney. Magn. Reson. Med. 67(1), 89–97 (2012)